Optics Letters

Cross-iteration deconvolution strategy for differential optical transfer function (dOTF) wavefront sensing

Fengyi Jiang,[1,2] Guohao Ju,[1,*] Xin Qi,[1,2] and Shuyan Xu[1]

[1]Changchun Institute of Optics, Fine Mechanics and Physics, Chinese Academy of Sciences, Changchun, Jilin 130033, China
[2]University of Chinese Academy of Sciences, Beijing 100049, China
*Corresponding author: juguohao@ciomp.ac.cn

Received 12 June 2019; revised 28 July 2019; accepted 29 July 2019; posted 1 August 2019 (Doc. ID 369717); published 23 August 2019

Differential optical transfer function (dOTF) is a promising analytic image-based wavefront sensing approach, which is simple in both hardware implementation and mathematical operation. However, there is one deep-rooted problem inherent in this approach, i.e., the essential trade-off between the signal ratio and resolution due to the effect of convolution. In this Letter, a cross-iteration deconvolution strategy is proposed to solve this problem with two different dOTFs, based on the understanding of an underlying prior knowledge when pupil blockage is used to introduce pupil modification. This Letter contributes to the development of a deterministic, efficient, and precise image-based wavefront sensing technique.

https://doi.org/10.1364/OL.44.004283

Differential optical transfer function (dOTF) is a new and promising image-based technique for measuring the complex pupil field (phase and amplitude) of an optical system. Unlike other image-based wavefront sensing methods, such as phase retrieval which involves Gerchberg–Saxton iterative transformation or iterative nonlinear optimization [1,2], the dOTF algorithm is analytic and non-iterative. This method is particularly suitable for the phasing of extra-large segmented space telescopes. It can directly determine the phasing errors (piston and tip-tilt) of all segments through a simple mathematical operation, while it is very hard for the iterative phase retrieval algorithms to search the true set of phasing error parameters, especially when the number of segments is particularly large.

The principle of the dOTF wavefront sensing approach is shown in Fig. 1 [3–6]. It is, in principle, a diversity technique that works by collecting two star images with a localized modification introduced into the pupil of the telescope for one of the star images. The pupil modification can be in phase, amplitude, or both. The collected two point spread function (PSF) images are Fourier transformed and subtracted from each other, resulting in a dOTF. The obtained dOTF includes the estimate of the complex field over the majority of the pupil, along with a second complex conjugated field image reflected about the location of the pupil modification.

However, there is one deep-rooted problem inherent in this method, i.e., the essential trade-off between the intensity of the dOTF signal and the resolution of the recovered complex pupil field. In effect, the complex pupil field included in the dOTF is blurred by convolution with the complex conjugate of the pupil modification. Considering that the OTF can be expressed as auto-correlation of the pupil field, the dOTF can then be given by

$$\mathrm{dOTF} = (\psi + \delta\psi) \otimes (\psi + \delta\psi)^* - \psi \otimes \psi^*, \tag{1}$$

where $\otimes$ represents correlation operation, and $*$ means the complex conjugate; ψ is the pupil field, and $\delta\psi$ is the pupil modification. Equation (1) can further be rewritten as

$$\mathrm{dOTF} = \psi \otimes \delta\psi^* + \psi^* \otimes \delta\psi + \delta\psi \otimes \delta\psi^*. \tag{2}$$

We can see that the dOTF includes three overlapping terms. Each term is a correlation between two field factors: either the unmodified pupil field (ψ) or the pupil modification ($\delta\psi$). Cross-correlating the pupil modification with the pupil field blurs the result and limits the spatial resolution of recovered wavefront phase map.

Therefore, it seems that a smaller modification area will be preferred if a higher resolution of the recovered wavefront map

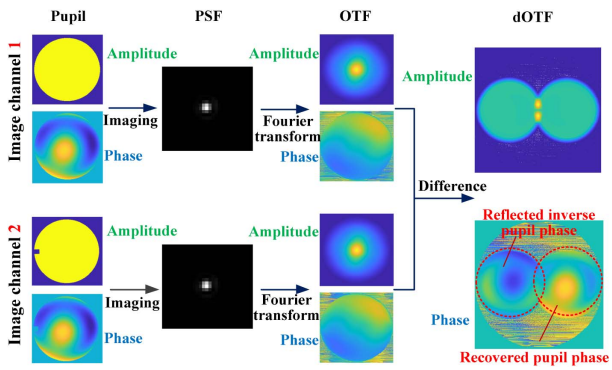

Fig. 1. Illustration of the principle of the dOTF wavefront sensing method.

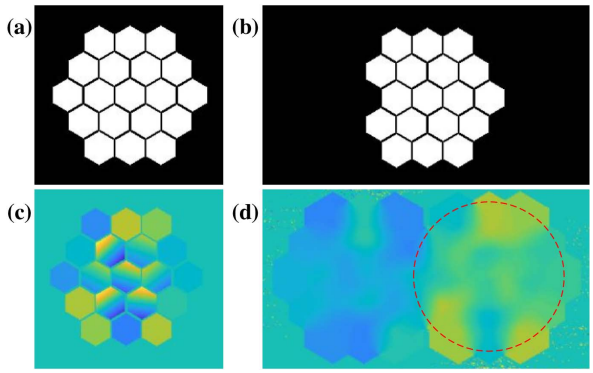

Fig. 2. Illustration of the blurring effect due to convolution inherent in the dOTF method. (a) shows the magnitude of the original pupil function for a segmented telescope. (b) shows the magnitude of the modified pupil function needed in the dOTF method. (c) shows the phase of the original pupil function, and (d) shows the recovered phase. We can see that the recovered phase is very blurred, and the accuracy is low.

is required. However, a smaller modification area also means a smaller change in OTF and, thus, a lower signal of dOTF will be obtained, which can easily be submerged by image noise (photon and detector noise are always present). Taking this fact into consideration, in practice, we have to increase the area of the modification in the pupil to increase the signal-to-noise ratio (SNR) of the dOTF, while the resolution (or accuracy) of the recovered wavefront phase map is restricted due to the blurring effect inherent in this method.

The blurring effect due to convolution is illustrated in Fig. 2. Here we are supposing that the dOTF is used to sense the phasing error of a segmented telescope. Pupil modification is introduced by blocking one segment near the edge of pupil. Comparing the original phase shown in Fig. 2(c) and the phase of the dOTF complex field (i.e., the recovered phase), we can see that the recovered phase is very blurred, and the resolution of the recovered phase is greatly decreased. Therefore, the dOTF method cannot be directly used for high-resolution phase recovery.

Fortunately, we can overcome this blurring problem using the technique of deconvolution. Previously, a deconvolution method was introduced to undo the detrimental effects of the extended pupil field change [7], and simulations are performed to demonstrate the effectiveness of it. However, the premise of this deconvolution method is the accurate knowledge of the complex pupil modification, which is actually unknown to us in practice. While it may seem that we can introduce a known phase change with a known piston or tip-tilt change of a sub-aperture, in effect, the complex pupil modification is still not known. Suppose that we use the vector $\vec{p} \equiv Ae^{i\theta}$ to represent an unknown complex number (A is the magnitude and θ is the azimuth angle). Even if the phase change, $\Delta\theta$, is known to us, we still do not know the change of this complex number, $\Delta\vec{p}$ ($\Delta\vec{p} \equiv Ae^{i(\theta+\Delta\theta)} - Ae^{i\theta}$). Therefore, at present, this deconvolution method can hardly be applied to practical situations.

In this Letter, we propose a novel deconvolution strategy without the need for accurate knowledge of the complex pupil modification in advance. The first important step is choosing a suitable type of pupil modification. In this Letter, the pupil modification is introduced by blocking a portion of the pupil near the edge of it. The most important reason for why we use transmission blockage rather than local phase change to introduce dOTF pupil change is that the complex field of pupil modification has inherent relations with sn unmodified pupil field in the area of pupil modification. The pupil field of the modification area after blocking becomes zero and, therefore, the complex field of pupil modification (the difference between the modified pupil field after blocking and the unmodified field) is the opposite of the unmodified pupil field in the area of pupil modification, i.e.,

$$\delta\psi(\rho_x, \rho_y) = \begin{cases} -\psi(\rho_x, \rho_y), & \text{if } (\rho_x, \rho_y) \in D, \\ 0, & \text{if } (\rho_x, \rho_y) \notin D, \end{cases} \tag{3}$$

where (ρ_x, ρ_y) represents the coordinate position of a point in the pupil plane, and D represents the area of pupil blockage. Revealing and understanding this underlying prior knowledge is the basis of our deconvolution method.

Then a cross-iteration strategy is further proposed for the deconvolution of the dOTF using an additional dOTF (which corresponds to a different pupil modification). The schematic diagram is shown in Fig. 3. The two different dOTFs can provide two estimated pupil fields with different regions of overlap. The pupil field in the second modification region can be estimated from the first dOTF. Then, utilizing Eq. (3), we can estimate the second complex pupil modification, which can be used for deconvolution of the second dOTF. Therefore, the first step of this strategy is to estimate the second complex pupil modification ($\delta\psi_2$) using the first dOTF according to Eq. (3), and perform deconvolution for the second dOTF. (The specific deconvolution process will be presented later.) Meanwhile, we suppose that we know the position and size of the blocked region, since pupil modification is usually artificially introduced by ourselves in practice. Note that the accuracy of $\delta\psi_2$ is affected by the convolution inherent in the first dOTF. Consequently, the performance of the first deconvolution is restricted. On the other hand, we can gradually

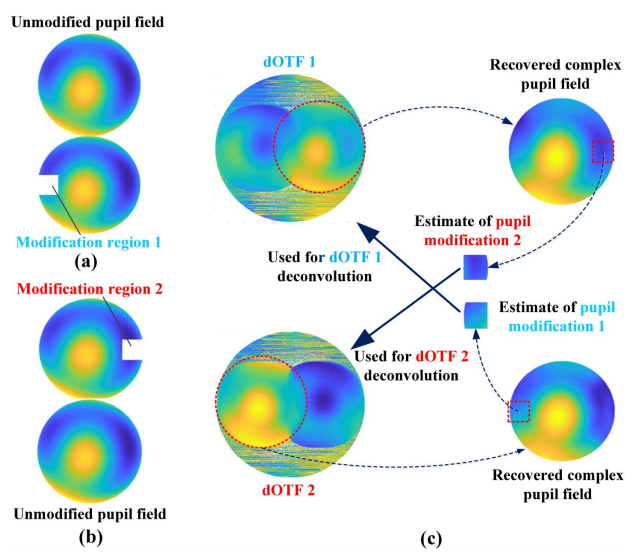

Fig. 3. Schematic diagram of the cross-iteration deconvolution strategy for dOTF wavefront sensing. The amplitudes of the pupil and OTF are not shown in this figure.

improve the performance of deconvolution in a cross-iteration form shown in Fig. 3. Therefore, the second step of this strategy is to estimate the first pupil modification ($\delta\psi_1$) from the initially deconvolved second dOTF according to Eq. (3), and perform deconvolution for the first dOTF. Then we will obtain a more accurate estimate of $\delta\psi_2$ from the deconvolved first dOTF, which contributes to the deconvolution of the second dOTF. This deconvolution process is iterative, but deterministic. After each iteration, the accuracy of the estimated pupil modification ($\delta\psi$) is improved which, in turn, leads to better performance of the subsequent deconvolution process. After several times of iteration, an accurate pupil field free from the effect of convolution can be obtained.

We continue to present the specific deconvolution process with an estimated pupil modification ($\delta\psi$). The deconvolution of the dOTF is better performed in the frequency space. Using Fourier transformation, Eq. (2) can be rewritten as [7]

$$\mathfrak{F}\{\mathrm{dOTF}\} = \Psi\delta\Psi^* + \Psi^*\delta\Psi + \delta\Psi\delta\Psi^*, \tag{4}$$

where $\mathfrak{F}\{\cdot\}$ represents Fourier transform operation, and Ψ and $\delta\Psi$ are the Fourier transforms of ψ and $\delta\psi$, respectively. Equation (4) can be rewritten as

$$\frac{\mathfrak{F}\{\mathrm{dOTF}\}}{\delta\Psi^*} = \Psi + \Psi^*\frac{\delta\Psi}{\delta\Psi^*} + \delta\Psi, \qquad (\delta\Psi^* \neq 0). \tag{5}$$

Then inverse Fourier transform is further performed, and we have

$$\mathfrak{F}^{-1}\left\{\frac{\mathfrak{F}\{\mathrm{dOTF}\}}{\delta\Psi^*}\right\} = \psi + \psi^* \otimes \delta\psi' + \delta\psi, \qquad (\delta\Psi^* \neq 0), \tag{6}$$

where

$$\delta\psi' = \mathfrak{F}^{-1}\left\{\frac{\delta\Psi}{\delta\Psi^*}\right\}, \qquad (\delta\Psi^* \neq 0), \tag{7}$$

Comparing Eq. (6) with Eq. (2), we can see that the pupil field ψ in Eq. (6) is no longer blurred by convolution with the complex conjugate of the pupil modification, $\delta\psi^*$. More specifically, in the region excluding the overlap area, ψ can be given by

$$\psi(\rho_x, \rho_y) = \mathfrak{F}^{-1}\left\{\frac{\mathfrak{F}\{\mathrm{dOTF}\}}{\delta\Psi^*}\right\}, \quad (\delta\Psi^* \neq 0, (\rho_x, \rho_y) \notin D). \tag{8}$$

In practice, we can use a mask to obtain ψ from the deconvolved dOTF.

In the presence of image noise, Eq. (5) should be modified; otherwise, the recovered phase will contain some random sharp peaks. According to the principle of Wiener filter, the term $1/\delta\Psi^*$ can be modified as [7,8]

$$\delta\Psi_W = \frac{1}{\delta\Psi^*} \cdot \frac{\delta\Psi^* \cdot \delta\Psi}{\delta\Psi^* \cdot \delta\Psi + 1/\mathrm{SNR}}, \qquad (\delta\Psi^* \neq 0), \tag{9}$$

where $1/\mathrm{SNR}$ is introduced to suppress the effect of noise near the nulls of the dOTF signal. Then Eq. (5) can be modified as

$$\begin{aligned}\bar{\Psi} &= \mathfrak{F}\{\mathrm{dOTF}\} \cdot \delta\Psi_W \\ &= \mathfrak{F}\{\mathrm{dOTF}\} \cdot \frac{1}{\delta\Psi^*} \cdot \frac{\delta\Psi^* \cdot \delta\Psi}{\delta\Psi^* \cdot \delta\Psi + 1/\mathrm{SNR}}, \quad (\delta\Psi^* \neq 0).\end{aligned} \tag{10}$$

In noise-free conditions, $1/\mathrm{SNR}$ is equal to 0, and the value of $\frac{\delta\Psi^* \cdot \delta\Psi}{\delta\Psi^* \cdot \delta\Psi + 1/\mathrm{SNR}}$ is equal to 1, i.e., Eq. (10) is the same as Eq. (5) in this case. In the presence of image noise, the term $1/\mathrm{SNR}$ can mediate the strong random sharp peaks, where the pupil modification is very small or even zero which will amplify the noise. Considering that it is difficult to obtain a certain SNR in practice, the selection of an appropriate parameter $\Gamma = 1/\mathrm{SNR}$ is the key to ensure the accurate recovered phase without random sharp peaks.

Note that in the cross-iterative deconvolution process the estimate of the pupil modification ($\delta\psi$) used for deconvolution of the corresponding dOTF is actually obtained from another dOTF with a different region of pupil modification. For example, in the deconvolution of dOTF 2, $\delta\psi_2$ is estimated using the first dOTF, according to Eq. (3):

$$\delta\psi_2(\rho_x, \rho_y) = \begin{cases} -\psi_2^{(1)}(\rho_x, \rho_y), & \text{if } (\rho_x, \rho_y) \in D_2, \\ 0, & \text{if } (\rho_x, \rho_y) \notin D_2, \end{cases} \tag{11}$$

where D_2 represents the region of the second pupil modification, and $\psi_2^{(1)}$ represents the pupil field in the region of second pupil modification estimated from the first dOTF.

To simulate noise, we model each image to have Gaussian CCD read noise with a standard deviation of $15e^-$ and a dark current of $0.1e^-/s$ over a 1 s integration time. The photon noise which is dependent on intensity follows a Poisson distribution. The peak pixel SNR (PSNR) is defined as

$$\mathrm{PSNR} = 20\log_{10}\left(\frac{S_{\mathrm{peak}}}{\sqrt{S_{\mathrm{peak}} + \sigma_{\mathrm{read}}^2 + \sigma_{\mathrm{dark}}^2}}\right), \tag{12}$$

where S_{peak} is the peak pixel value of the noise-free image, and σ_{read}^2 and σ_{dark}^2 are the variances associated with the readout noise and the dark current noise at each pixel, respectively.

Simulations will be performed to evaluate the effectiveness of the proposed cross-iteration deconvolution strategy in the noisy conditions. The peak of the PSF is set to 0.1 million photons, which is restricted to full well electron numbers. Then the final peak pixel PSNR is approximately equal to about 50 dB. In this case, the results of dOTF wavefront sensing with the proposed cross-iteration deconvolution strategy and Wiener filter are shown in Fig. 4. The residual root-mean-square errors (RMSEs) between the recovered phase and original phase during the cross-iteration deconvolution process are shown in Fig. 5. We can see that due to the presence of noise, the recovered phase map becomes a little rugged and blurred. However, the cross-iteration deconvolution strategy is still effective for a comparative large scale of phase aberrations (including piston and tip-tilts of each segment randomly selected in the range of $[-0.5\lambda, 0.5\lambda]$). The final RMSE is about 0.01λ. The convergence efficiency is high, even in the presence of image noise.

Monte Carlo simulations are further performed to validate the effectiveness of the proposed deconvolution method. On one hand, two different noise levels are considered, and the PSNRs for these two cases are 60 and 40 dB, respectively. For each case, 100 sets of piston and tip-tilt terms are randomly generated within the range of $[-0.5\lambda, 0.5\lambda]$. For each set of phasing errors, three PSFs corresponding to the full pupil and two different modified pupils are generated according to the principle of Fourier optics. These three PSFs are then used to recover the introduced phasing error with the proposed method. The results of the Monte Carlo simulations are shown

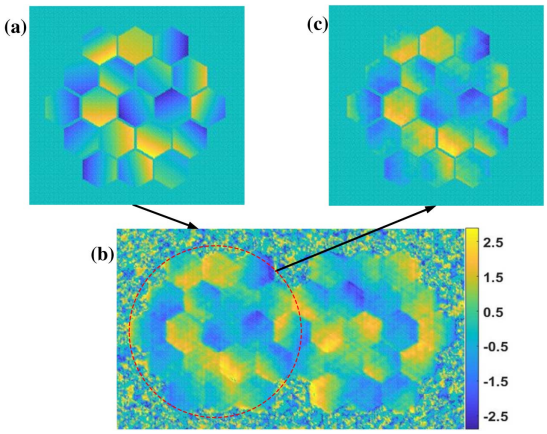

Fig. 4. Results of cross-iteration deconvolution in the noisy condition (PSNR ≈ 50 dB). (a) shows the original phasing errors of a segmented pupil. (b) shows one intermediate result of the dOTF phase during the cross-iteration process. (c) shows the final result after several times of cross-iteration. Comparing (a) and (c), we can see that the proposed approach is effective in noisy condition.

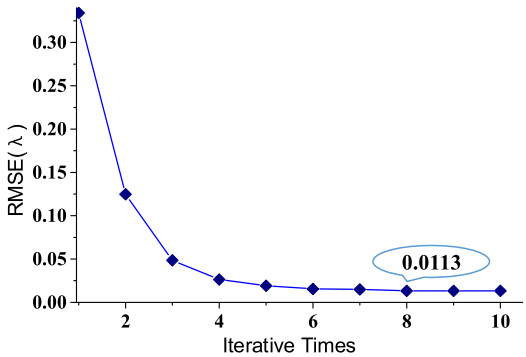

Fig. 5. Residual RMSEs between the recovered phase and original phase during the cross-iteration deconvolution process in the noisy conditions (PSNR ≈ 50 dB). We can see that the final RMSE after several times of iteration is about 0.01λ in the noisy conditions.

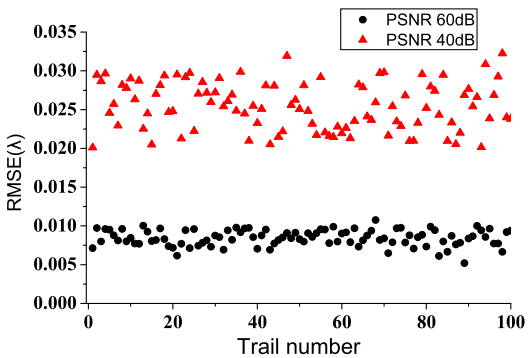

Fig. 6. Monte Carlo simulations for dOTF wavefront sensing with the proposed cross-iteration deconvolution strategy for the case of a high PSNR (60 dB) and the case of a comparatively low PSNR (40 dB). We can see that the proposed strategy can be applicable to both cases, while the accuracy actually decreases for the case of a low PSNR.

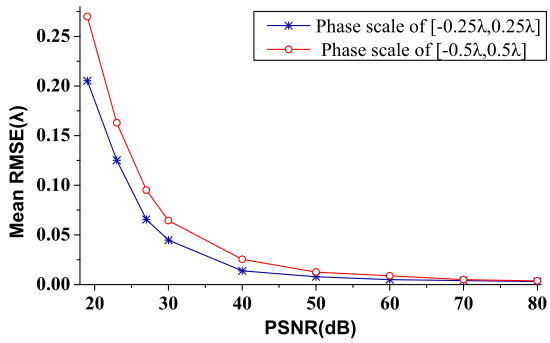

Fig. 7. Monte Carlo simulations for dOTF wavefront sensing with the proposed cross-iteration deconvolution strategy for different phase scales and different noise levels.

in Fig. 6. We can see that the proposed deconvolution method is effective for both of the cases, and an acceptable residual RMSE can be obtained.

On the other hand, we further demonstrate the effectiveness and accuracy of the proposed method for different phase scales and different noise levels. The results are presented in Fig. 7, which shows how the accuracy of the proposed approach changes with the phase scale and noise level.

To conclude, this Letter proposes a novel and efficient approach for deconvolution of dOTF wavefront sensing using two different dOTFS, without the knowledge of the complex field of pupil modification. The key step is revealing and understanding an underlying prior knowledge when pupil blockage is used to introduce pupil modification, i.e., the complex field of pupil modification is the opposite of the unmodified pupil field in the area of pupil modification. On this basis, a cross-iteration strategy is further proposed to gradually improve the performance of deconvolution. The cross-iteration deconvolution process is deterministic and has a high convergence efficiency. The effectiveness of the proposed approach has been validated for different phase scales (mainly including piston and tip-tilts of each segment) and different noise levels. It is shown that the accuracy is higher than 0.025λ when the PSNR is higher than 40dB. This Letter can greatly improve the resolution and accuracy of dOTF wavefront sensing and contributes to the development of deterministic, efficient, and precise image-based wavefront sensing technique.

Funding. National Key Research and Development Program (2016YFE0205000, 2016YFF0103603); National Natural Science Foundation of China (NSFC) (61905241, 61705223, 61805235).

REFERENCES

1. R. W. Gerchberg and W. O. Saxton, Optik **35**, 237 (1972).
2. R. A. Gonsalves, Opt. Eng. **21**, 829 (1982).
3. M. Hart and J. L. Codona, Proc. SPIE **8520**, 85200I (2012).
4. J. L. Codona, Opt. Eng. **52**, 097105 (2013).
5. J. L. Codona and N. Doble, J. Astron. Telesc. Instrum. Syst. **1**, 029001 (2015).
6. J. L. Codona and N. Doble, Proc. SPIE **8447**, 84476R (2012).
7. J. M. Knight, A. T. Rodack, J. L. Codona, K. L. Miller, and O. Guyon, Proc. SPIE **9605**, 960529 (2015).
8. R. Neelamani, H. Choi, and R. G. Baraniuk, IEEE Trans. Signal Process. **52**, 418 (2004).